Bioinsp. Biomim. **3** (2008) 016004 (11pp) doi:10.1088/1748-3182/3/1/016004

Assessment of bioinspired models for pattern recognition in biomimetic systems

G Pioggia[1], M Ferro[1], F Di Francesco[2], A Ahluwalia[1] and D De Rossi[1]

[1] Interdepartmental Research Center 'E Piaggio', University of Pisa, Italy
[2] Department of Chemistry and Industrial Chemistry, University of Pisa, Italy

E-mail: giovanni.pioggia@ing.unipi.it

Received 11 November 2007
Accepted for publication 20 February 2008
Published 10 March 2008
Online at stacks.iop.org/BB/3/016004

Abstract
The increasing complexity of the artificial implementations of biological systems, such as the so-called electronic noses (e-noses) and tongues (e-tongues), poses issues in sensory feature extraction and fusion, drift compensation and pattern recognition, especially when high reliability is required. In particular, in order to achieve effective results, the pattern recognition system must be carefully designed. In order to investigate a novel biomimetic approach for the pattern recognition module of such systems, the classification capabilities of an artificial model inspired by the mammalian cortex, a cortical-based artificial neural network (CANN), are compared with several artificial neural networks present in the e-nose and e-tongue literature, a multilayer perceptron (MLP), a Kohonen self-organizing map (KSOM) and a fuzzy Kohonen self-organizing map (FKSOM). Each network was tested with large datasets coming from a conducting polymer-sensor-based e-nose and a composite array-based e-tongue. The comparison of results showed that the CANN model is able to strongly enhance the performances of both systems.

1. Introduction

The new breakthroughs made in the past few decades in material science in order to develop intelligent materials allow one to mimic the nature of biological systems in terms of sensing and actuation capabilities [1]. In the early 1980s, Persaud and Dodd [2] first established that an array of non-selective sensors could be used to discriminate between simple odors through pattern recognition schemes. These advances allowed devices such as electronic noses (e-noses) and tongues (e-tongues) to become widespread [3]. Artificial noses and tongues have numerous applications [4, 5], such as the monitoring of emissions of outdoor [6] or indoor [7] volatile organic compounds and the detection of explosives [8], and several sensing systems have been commercialized. The principal application of e-noses is in the food and agricultural fields [9, 11], i.e. inspection of food, grading quality of food, fish inspection, fermentation control, beverage container inspection, automated flavor control, and so on, although recently several other areas have been suggested [12]. An electronic nose could also have applicability as a diagnostic tool [13]. An electronic nose could examine odors from the body (i.e. breath, wounds, body fluids, and so on), identifying possible problems. Odors in the breath can be indicative of diabetes, breast cancer, lung cancer and heart transplant rejection [14–20].

Systems capable of discriminating liquid-phase tastes have been slower to follow, although recently several artificial tongues have been proposed [21]. Taste sensors have mainly been utilized to discriminate between various brands of food and drink, and most of the work in this area has been pioneered by a Japanese group [22] who have assessed a whole range of liquids and semi-liquids such as water, sake, beer and tomatoes. Their sensors are composed of a variety of lipids in a polymer matrix which respond by changing their potential in the presence of different liquids. More recently, other research groups have also developed electronic tongues [23–25]. Vlasov's system is based on an array of chalcogenide glass electrodes which have a broadband sensitivity to cations and anions whilst Lundstrom's group have reported a system using metal electrodes based on pulsed voltammetry.

At present, these instruments often fail to give the expected results and the research is under development. This happens for a series of concomitant causes, ranging

from the measurements, to the limits relevant to instability and non-reproducibility of most existing sensors, up to the inappropriate use of the pattern recognition scheme. Pattern recognition techniques are used to analyze data with the aim of reproducing typical olfactory and gustative system functions, such as the perception of an odor/taste and its classification through the comparison with similar stimuli perceived in the past. Many techniques are used for this purpose, but recently, the e-nose and e-tongue processing architectures are often performed by models inspired by biology, such as genetic algorithms and artificial neural networks (ANN) [26–30]. Such architectures require high-efficiency interconnection and cooperation of several heterogeneous modules, i.e. control, data acquisition, data filtering, feature selection and pattern analysis [31].

In this paper, the raw signals obtained from an e-nose and an e-tongue were pre-processed in order to extract relevant features, such as the energy, the absolute maximum value, angular coefficients and steady-state values. The feature vectors constitute the data set for the pattern recognition processes. The pattern recognition was performed by a cortical-based artificial neural network (CANN) and the results were compared with the performances of a multilayer perceptron (MLP), a Kohonen self-organizing map (KSOM) and a fuzzy Kohonen self-organizing map (FKSOM) [37–40]. Each network was tested with the same data sets coming from the e-nose and e-tongue. Data from the e-nose were acquired during the analysis of 45 different olive oil samples and data from the e-tongue were acquired during the analysis of five compounds able to elicit different kinds of gustative perceptions (glucose, sodium dehydrocholate, sodium chloride, citric acid and glutamic acid) corresponding to the five classic tastes. In the CANN an artificial neuron model with high computational efficiency and biological accuracy was adopted. Such a model, recently proposed by Izhikevich [42, 43], takes 13 floating point operations (FLOPs) to simulate 1 ms of neuron activity. The theory of neuronal group selection (TNGS) [44] proposed by Edelman was adopted as the learning strategy of the CANN. The TNGS considers the selection as the basis for the learning process. To take into account this theory the time variable in the learning task was used, so that neural groups may arise from a selection process. The network design was inspired by the anatomical structure found in a layer of the mammalian cortex.

2. Artificial implementation of chemical senses

An artificial nose or tongue can be divided into three main units, each of which plays an essential role in the recognition process: an array of broadband sensors; the transduction, hardware and processing systems; the pattern recognition and classification tools.

2.1. The e-nose

2.1.1. Sensors. In this work, conducting chemo-sensitive layers, which change their electrical conductivity in the presence of volatiles, obtained by the deposition of suspensions of chemically doped alkoxy-substituted polythiophenes, namely poly-(3,3'-dipentoxy-2,2'-bithiophene), were used. Alkoxy-substituted polythiophenes were selected as conducting polymers due to the low potential for oxidation and to the great stability of the conducting state. A controlled doping with salts enables them to be conductive. This process complies with the development of a wide variety of sensors, whose response depends on the degree of affinity between volatile and the doped polymer. Preparation and characterization of chemo-sensitive layers based on alkoxy-substituted polythiophenes exposed to organic vapors have previously been reported [34]. Since electric resistance is the parameter chosen to evaluate the sensors' response, it was also used to monitor the sensor stability over time. As shown in figure 1, sensors are generally stable after a stabilization phase of about 10 days (variation percentage of resistance value less than 5%). A typical response of a sensor to a series of different concentrations of benzene (increasing concentrations from 1000 ppm to 30 000 ppm) is shown in figure 2. An evaluation of sensors' selectivity was obtained by measuring the resistance variations during the exposure to saturated organic vapors (figure 3). The measurement protocol consisted of three phases for each experiment: baseline acquisition, i.e. sensors flushed with nitrogen, exposure, i.e. sensors exposed to the sample, and finally desorption and cleaning, i.e. volatiles flushed with nitrogen to restore baseline conditions. In figure 3, the abscissa shows the steady-state resistance variation between exposure and baseline during the exposure to volatiles; they are listed in the ordinate according to the magnitude of response. The sensors were exposed to volatiles in a random order.

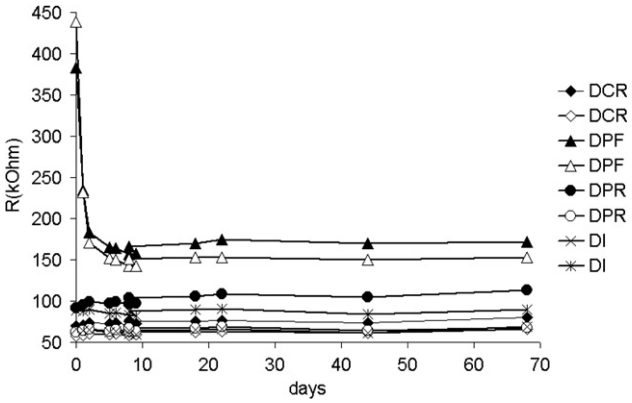

Figure 1. Sensors' stability. Legend: different sensor codes.

2.1.2. The experimental set-up. In order to expose volatiles to the chemo-sensitive layers, a sampling system devoted to collecting and conveying volatile samples generated by the headspace of organic compounds was realized. The headspace is generated within 125 ml glass vials containing 10 ml solutions (2.5 μl ml^{-1}) of liquid samples. The instrument (figure 4) conveys a volatile sample, by means of a gas carrier such as nitrogen or pure air, into an exposure chamber where the sensors are lodged. The aim of the chamber is to expose an array of sensors to volatiles in optimal conditions. The sensors

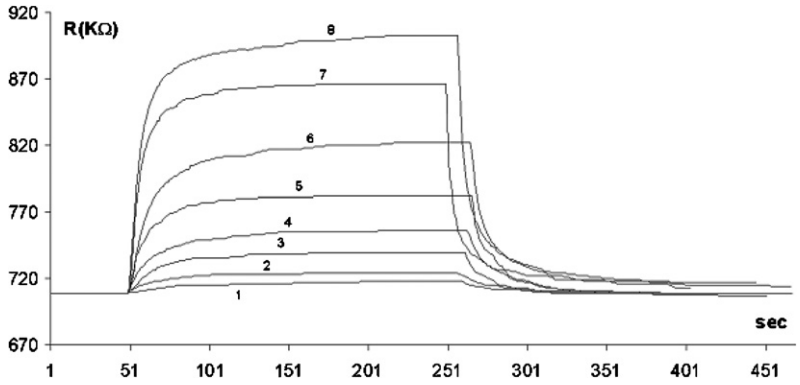

Figure 2. A typical response of a sensor to a series of different concentrations of benzene.

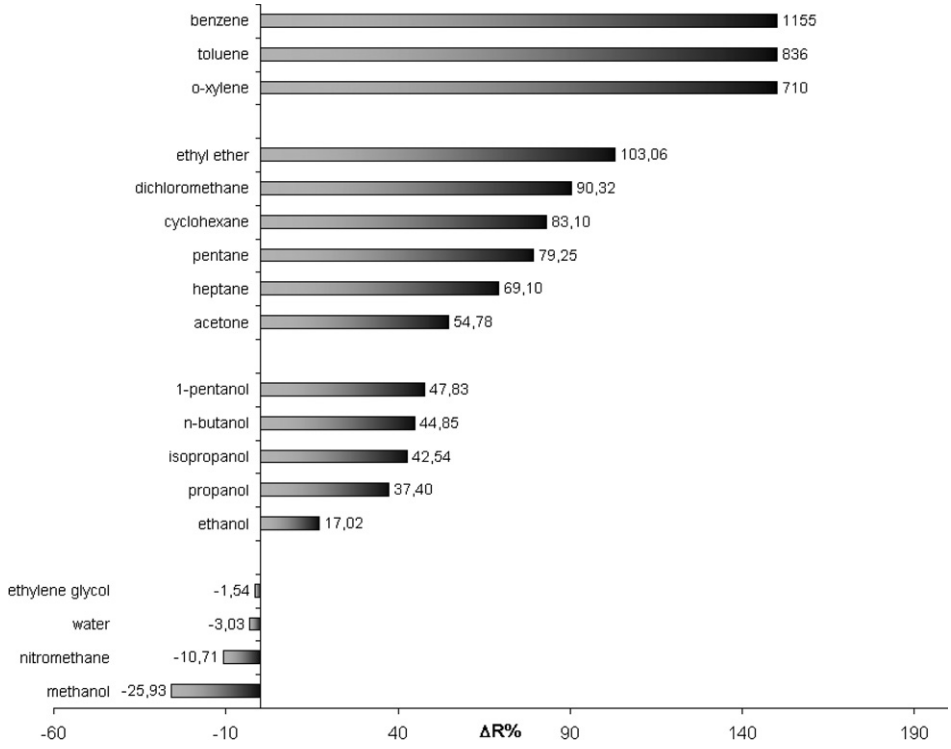

Figure 3. Sensors' selectivity.

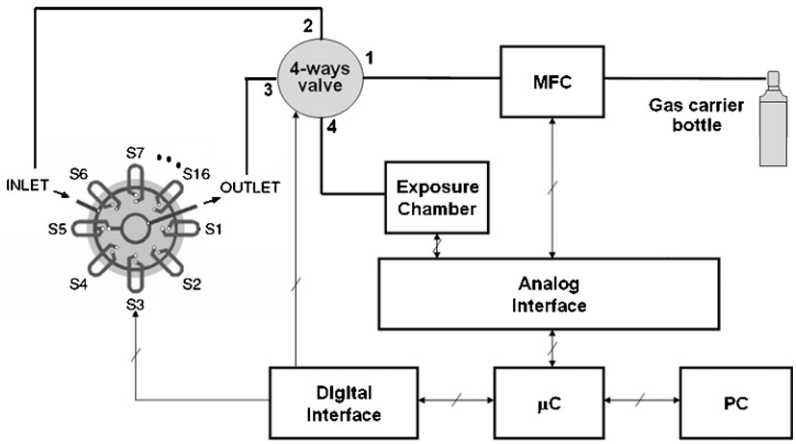

Figure 4. E-nose experimental set-up.

are housed in an eight-sensor stainless steel exposure chamber. In order to expose an array of sensors to a chemical mixture in optimal conditions, the chamber must allow all the sensors to be simultaneously exposed under the same conditions. This makes it possible to accurately reproduce the shape of the input concentration signal at each sensor position. Moreover, it must be designed to obtain the same concentration profile in repeated measurements and short analyte concentration rise/fall times, to avoid memory effects and sample dilution. A homogeneous flow with a low speed gradient, no recirculating zones or stagnant regions and the same local concentration of volatiles over each sensor were obtained by choosing a radially symmetric geometry for the chamber with a dedicated deflector which allows homogeneous flow conditions with low velocity gradients. The measurement protocol consists of three phases for each experiment: baseline acquisition (sensors are flushed with nitrogen); exposure (sensors are exposed to the sample headspace); desorption and cleaning (odors are flushed away by nitrogen to restore baseline conditions).

2.1.3. Hardware architecture. The hardware architecture consists of an electronic section able to perform fast and accurate measurements with a conductive polymer sensor array and to perform a dynamic and automatic control of the sampling process [31]. The electronic section consists of a central processing unit, an analog interface and a digital interface. The analog interface can drive up to 16 sensors with a resistance of the sensing layer within the range of 500 Ω–1 MΩ. Shielded cables connect each sensor to the analog interface. For each sensor a different current can be selected and injected thanks to 16 independent digital current generators. Each current generator is realized with a 12 bit D/A converter, with a resolution of 1.22 μA bit^{-1}, which allows 4096 different currents to be chosen. The analog interface includes the electronics for controlling an array of mass flow controllers and the temperatures of two external devices. The acquisition of the sensor transduction signals is performed by 16 independent 24 bit delta–sigma differential analog-to-digital converters with a resolution of 298 nV bit^{-1}. The digital interface includes a 32 bit microcontroller, a 2 MB non-volatile memory for data and a 1 MB flash memory for system configuration. Moreover it includes the electronics for driving the above-mentioned experimental set-up. A dedicated firmware allows the microcontroller to manage the electronic and the hydraulic sections. A communication protocol was designed to allow a personal computer to control the microcontroller tasks. A framework controls the synchronization of the data flow between the microcontroller and the personal computer through a framework I/O interface. The framework I/O interface has been developed in order to act as a buffer for the flow of information coming in and out of the microcontroller.

2.2. The e-tongue

The current research in electronic tongues is based mainly on electrochemical measurements, with the main focus being on the development of novel sensors, such as membranes and

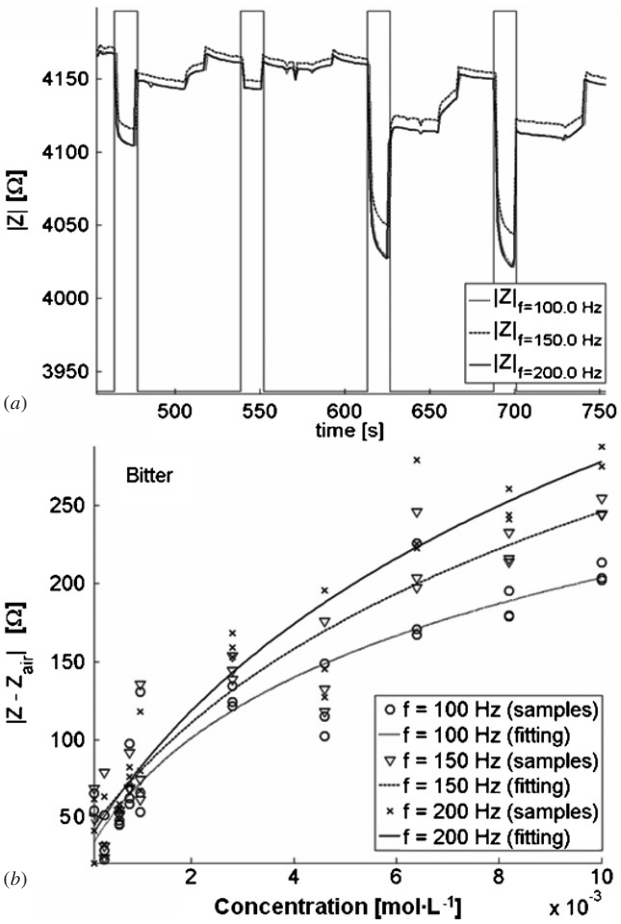

Figure 5. (*a*) Typical e-tongue sensor responses; (*b*) PCL-CNT sensor responses to bitter compounds at the three different frequencies.

electrode coatings. Indeed, the use of impedance measurement represents a novel approach for the realization of an electronic tongue [32]. This approach is justified by the affinity with the measurement of resistance variations which is the most commonly used method for electronic noses.

2.2.1. Sensors. Three different sensing layers were used. The first sensing layer consisted of polycaprolactone (PCL) loaded with carbon nanotubes (CNTs). The second sensing layer was realized from a matrix of polylactic acid (PLA) loaded with carbon black and it is based on the method described by Lonergan *et al* [33]. In the third case, a sensing layer consisting of poly(alkoxy-bithiophenes), previously prepared and characterized from the authors in response to organic vapors [34], was adopted.

The responses of the PCL-CNT sensor to bitter, salty and sour compounds at the three different frequencies (100 Hz, 150 Hz and 200 Hz) are shown in figures 5 and 6. The data show that sodium chloride and citric acid are easily recognized and distinguishable even at the lowest concentrations. Glutamic acid and sodium dehydrocholate have acceptable errors too, of the order of a few %, with 200 Hz giving rise to the lowest errors for these two compounds.

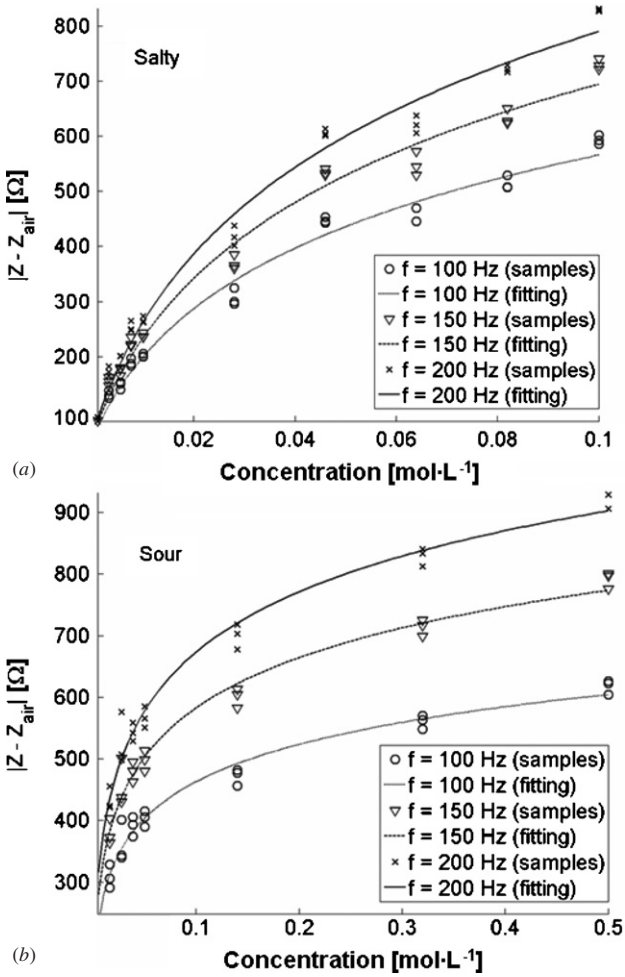

Figure 6. (*a*) PCL-CNT sensor responses to salty compounds at the three different frequencies; (*b*) PCL-CNT sensor responses to sour compounds at the three different frequencies.

Glucose also had a large fitting error, confirming that the sensor was unable to adequately distinguish this compound at all frequencies for the selected concentrations. A linear relation between impedance and concentration was found with respect to the umami taste; therefore the sensor can interact with this compound and distinguish between different concentrations. Although the logarithmic equation used was quite arbitrary, there is a good correlation between the fitting error and the ability of the sensors to distinguish and discriminate substances and concentrations.

2.2.2. The experimental set-up. An automated measurement system composed of an impedance meter, a mechanical arm, a rotating platform and a data acquisition card was designed and realized (figure 7). The rotating platform was capable of housing up to six beakers simultaneously, which were filled with five solutions under test and the rinsing deionized water. A multiplexer allowed the sequential scanning of the sensors for the impedance measurement, while the array was automatically dipped into the baseline and test solutions by

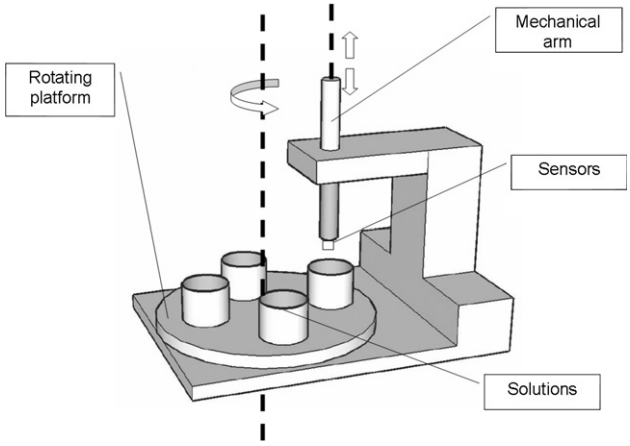

Figure 7. e-tongue experimental set-up.

the coordinated movements of mechanical arm and rotating platform. The following protocol was adopted: sensors in air (start of data acquisition); sensors dipped in distilled water; sensors in air; sensors in solution 1; new cycles (a)–(d) for the other solutions; sensors in air (stop acquisition); baseline acquisition (sensors in air); exposure (sensors dipped in the selected solution); desorption and cleaning (sensors in air; sensors dipped in deionized water).

2.2.3. Hardware architecture. The electric impedance of the sensor array was monitored at a frequency of 150 Hz. At much higher frequencies, the impedance converges to a single value independent of the sensor composition and only related to the conductivity of the system, whereas at lower frequencies the system is slow and subject to ambient noise. The slope of the impedance spectrum at around 150 Hz is maximum, and this frequency was thus selected as the most sensitive, capable of guaranteeing the best discrimination. A power supply generates a 150 Hz sinusoidal voltage which is sent to a voltage–current converter. The converter outputs a constant current that flows in a reference resistance and in the sensor. The resulting voltage at the two ends of the reference resistance is collected by a differential amplifier and is used as the reference voltage. Another differential amplifier collects the voltage at the two ends of the sensor, which will result in a signal with different modulus and phase with respect to the reference voltage. Such an analog signal is then converted, acquired and processed by a PC equipped with a data acquisition electronic board (National Instruments PCI6023E).

2.3. Software architecture

The software architecture has been designed as a hierarchical structure whose root is a manager module. Several application processes run inside its core, acting on the dataset available in the framework I/O buffer. The framework is able to control all the modules of the elaboration chain, including analysis protocol management and interfaces. During a signal pre-processing stage various purposes are served, including

baseline manipulation, compression, normalization and drift compensation. Afterwards, data are sent to a dimensionality reduction module in order to perform a feature extraction. Selected features are ready for analysis, classification and clustering tasks. A process devoted to data normalization gets sensory data from the framework I/O interface. Normalized data are sent to a process devoted to feature extraction in order to build the data set. Different pattern recognition processes described in the following sections perform the data set classification task. A process devoted to the evaluation of the pattern recognition by means of cross-validation shows the classification results.

2.3.1. Features extraction. As regards the signals coming from the artificial olfactory system, let $x_n^k(t)$ be the resistance versus time t of the nth of N sensors as the response to the kth of K samples. $x_n^k(t)$ signals were windowed and normalized over the exposure time, i.e. the samplings were selected within the time interval $L = (t_1, t_2)$, resulting in the function $\overline{x_n^k}(t) = x_n^k(t)/(x_{\min}^k - 1)$, where $x_{\min}^k$ represents the minimum value of $x_n^k(t)$ in the time interval L. A set of F features from the normalized signals was extracted; let $f_{n_1}^k, \ldots, f_{n_F}^k$ be the features. The features were: the energy, i.e. $E_n^k = \sum_{i \in L} \overline{x_n^k}(t)^2$; the absolute maximum value; the angular coefficient of the line connecting $\overline{x_n^k}(t_1)$ and $\overline{x_n^k}(t_{\max})$; the angular coefficient of the line connecting $\overline{x_n^k}(t_{\max})$ and $\overline{x_n^k}(t_2)$. Thus a data set, where each response can be represented as a point in $\Re^{K \times F}$, was obtained. The features were normalized in the 0–1 interval.

As regards the e-tongue, the data were collected in a database, then suitable queries allowed the extraction of the steady-state impedances of sensors. The features were the normalized magnitude and phase of the steady-state impedances.

2.3.2. Pre-processing. Before applying any classification technique, the identification and the removal of outliers (samples significantly different from analogues belonging to the same population) was needed. As samples of each category were obtained in our case by replicates of the same measurement procedure, a multivariate normal distribution around an ideal category representative might be expected, deviations from that point being due to experimental errors. Large deviations may be generated by random errors either in the sample preparation and measurement or in the data acquisition and treatment, so that it is not possible to consider the resulting object a typical sample of that category. Principal component analysis (PCA) [35] was used to display data and detect outliers, by using the Q and T^2 diagnostics. Samples identified as outliers for at least one of these statistics with $p < 0.001$ (more than three standard deviations from the mean value of any category) were removed.

3. Pattern recognition models

In e-noses and e-tongues, the pattern recognition task is often performed by using ANNs [27]. The concept of ANNs is to imitate the structure and workings of the human brain by means of mathematical models. ANNs possess an adaptable knowledge that is distributed over many neurons which can communicate (locally) with one another. The structure of the single neuron model, the network topology and the adaptation (learning rule) define the ANN architecture. The neurons (processing units) are single elements and consist principally of a connection function, an input function, an activation (transfer) function and an output function. A neuron receives signals via several input connections. These are weighted at the input to a neuron by the connection function. The weights define the coupling strength (synapses) of the respective connections and are established via a learning process, in the course of which they are modified according to given patterns and a learning rule. In the case of supervised learning, in addition to the input patterns, the desired corresponding output patterns are also presented to the network in the training phase. In the case of unsupervised learning, the network is required to find classification criteria for the input patterns independently. Stochastic learning methods employ random processes and probability distributions to minimize a suitably defined energy function of the network. A large number of neural models now exist, and each of these models is available in various forms. The Integrand-and-Fire (IF) neuron model [37] is often used in to create ANNs suitable for classification and forecast tasks. However when dealing with ANNs, as shown by Goodner *et al* [36], the risk of data over-fitting can lead to counterfeit classifications. According to these authors the ratio between samples and variables should be greater than 6 in order to obtain reliable results.

3.1. Multi-layer perceptron (MLP)

The multi-layer perceptron (MLP) [37] is a type of neural network, where the IF neuron model is adopted, allowing representation of the relations between input and output values. This type of network is trained with the help of a supervised learning method, i.e. input and output values are specified and the relations between them are learnt. The neural network approximates every nonlinear mapping of the form $y = f(x)$. Every data record consists of input data and the corresponding output data. The MLP learns the input/output behavior of the system examined via a training data set.

In the training phase, for each data record, each activation function of the artificial neurons is calculated. The weight w_{ij} of a generic neuron i at the time T, for the input vector $\overline{f_n^k} = f_{n_1}^k, \ldots, f_{n_F}^k$, is modified on the basis of a well-established technique, the propagation of the resulting error between the input and the output values. The response of the MLP is a Boolean vector; each element represents the activation function of an output neuron. After the training process, the performance of the classification task is commonly evaluated using the confusion matrix [38]. The generic element r_{ij} of the confusion matrix indicates as a percentage how many times a pattern belonging to the class i was classified as belonging to the class j. A more diagonal confusion matrix corresponds to a higher degree of classification. Since each pattern may be confused with more than 1 pattern, the sum

on each row and column may differ from the value of 100%. In order to check the generalization capability of the neural network, a cross-validation process is carried out.

3.2. Kohonen self-organizing maps (KSOM)

A Kohonen self-organizing map (KSOM) [39] maps the original space into a two-dimensional net of neurons in such a way that close neurons respond to similar signals, in order to solve classification tasks and to find structures in data. KSOMs are unsupervised neural networks, i.e. they exploit similarities of samples apart from the class which they belong to. In the unsupervised training process, the synaptic weight vectors of the artificial neurons of the KSOM are adapted by means of the training data set examples in such a way that the KSOM supplies as good a representation as possible for the training data set. The synaptic weight vector of an artificial neuron of a KSOM corresponds to the feature vector of an object in the feature space under study. In a KSOM, a *winner-takes-it-all* training algorithm is performed. In this work the IF neuron model was adopted. It is worth mentioning that the KSOM learns to discriminate in such environmental conditions; therefore, in the case of uncontrolled environmental parameters, a new data set for each measurement campaign is needed. For each input vector, the neuron that has the minimum distance $d = \min_i \|\overline{f} - w_i\|$ from the input vector is the winning unit z. The weight w_{ij} of a generic neuron i at the time T, for the input vector $\overline{f_n^k} = f_{n_1}^k, \ldots, f_{n_F}^k$, is modified as follows [39]:

$$w_{ij}(T) = w_{ij}(T-1) + \alpha(T) r_{iz}(T)[\overline{f}_j(T) - w_{ij}(T-1)],$$

where $\alpha(T) = f_\alpha \alpha(T-1)$ is the learning rate with a learning rate factor, $r_{iz}(T) = \mathrm{e}^{-\frac{d^2}{\sigma^2}}$ is the feedback function of the neuron i to the winning neuron z, and $\sigma(T) = f_\sigma \sigma(T-1)$ is the learning radius with the learning radius factor f_σ.

The response of the KSOM is a Boolean vector; each element represents the activation function of a neuron. After the training process, a supervised labeling step is performed. Cluster labels are assigned to the individual artificial neurons. This is done via the interpretation of the content of the synaptic weight vectors (feature vectors) of the artificial neurons. Here the same label can be assigned to several artificial neurons so that the cluster can be represented by several artificial neurons. After validation of the KSOM by examples of a test data set, the performance of the classification task is commonly evaluated using the above-mentioned confusion matrix. In order to check the generalization capability of the neural network, a cross-validation process is carried out. In this work, we fixed the parameters $\alpha(T) = 0.8$, $f_\alpha = 0.85$, $\sigma(0) = 5$, $f_\sigma = 0.9$ and a training of 5000 epochs, which allows one to obtain the best performance of the network for the above-mentioned artificial olfactory and gustative systems.

3.3. Fuzzy Kohonen self-organizing maps (FKSOM)

A fuzzy Kohonen self-organizing map (FKSOM) [40] combines characteristics of the fuzzy C-means algorithm [41] and the above-mentioned Kohonen network. An unsupervised learning method is used. FKSOM can represent any desired class forms in the feature space. Classification is unambiguous, i.e. one classified object is assigned to exactly one class. In the learning phase, however, the fuzzy C-means algorithm is used to optimize the learning process. Fuzzy C-means is a fuzzy cluster method, suitable for classification tasks, which determines the class prototypes for an existing data set and a specified number of classes. Each of the so-called cluster centers represents the typical object for one class. The fuzzy C-means algorithm assigns a classification of 0 to 1 between each object to be classified and each class. This method allows hypersphere-shaped classes to be found in a multi-dimensional feature space. An object to be classified is described by the input vector $\overline{f_n^k} = f_{n_1}^k, \ldots, f_{n_F}^k$. No information on class assignment is required for clustering as it is an unsupervised learning method. Classification is based on the calculation of a distance. After the training process, a supervised labeling step is performed; the performance of the classification task is commonly evaluated using the confusion matrix and a cross-validation process.

3.4. The cortical-based artificial neural network (CANN)

The complexity of a biological neuron may be reduced by using several mathematical models. Each of these reproduces some of the functionalities of real neurons, such as the excitability in response to a specific input signal. The most accurate model for a biological neuron has been developed by Hodgkin and Huxley [45]. Such a model is able to exactly reproduce the shape of the action potential of a neuron by taking into account the involved ionic currents, but it is computationally expensive. It takes about 1200 FLOPs to simulate 1 ms of a single neuron activity. Several attempts have been made in order to reduce the mathematical complexity of a neuron model: the Morris–Lecar model [46], still close to the Hodgkin–Huxley model, takes about 600 FLOPs for 1 ms of neuron activity, while the FitzHugh and Nagumo model [47] takes about 72 FLOPS for 1 ms of neuron activity. Izhikevich [42, 43] recently developed a simple model for an artificial neuron which is able to reproduce almost all the functionalities of the biological neurons. The model, consisting of two differential equations with four parameters, takes 13 FLOPs to simulate 1 ms of neuron activity. In this work, the Izhikevich model was used and the spike-timing-dependent plasticity (STDP) rule [48], which permits the implementation of a learning rule based on patterns which continuously flow from a data set, has been adopted according to the TNGS of Edelman [44].

3.4.1. The artificial neuron model. In the CANN, the artificial neuron model proposed by Izhikevich [45] was adopted. The model is given by:

$$\begin{cases} v' = 0.04v^2 + 5v + 140 - u + I \\ u' = a(bv - u) \end{cases}$$

with the condition:

$$\text{if } v \geqslant +30\,\text{mV}, \qquad \text{then} \begin{cases} v \leftarrow c \\ u \leftarrow u + d. \end{cases}$$

The four parameters (a, b, c and d) are dimensionless values. The v variable represents the membrane potential of the neuron, while u takes into account the activation of K^+ ionic currents and the deactivation of the Na^+ ionic currents. The I variable takes into account the synaptic currents and the bias currents as the input signal of the neuron. Depending on the values of the four parameters, the system may have a steady state (which corresponds to a lack of activity in the neuron) and an unsteady state (which corresponds to the presence of activity in the neuron). The reset condition is needed to perform the return of the system into the steady state after the neuron has fired.

3.4.2. Selection of neuronal groups. The TNGS proposed by Edelman [44] suggests a novel way for understanding and simulating neural networks. The time variable is taken into account in the learning task, so that neural groups may arise from a selection process. The correspondence between synaptic weights and axonal delays exists as a result of the neuron behavior. One neuron can belong to many groups, whose count is usually higher than the count of the neurons in the map. This guarantees a memory capability which is higher than the capability reached by the classical artificial neural networks. The classical approach in ANN simulation takes into account the modulation of the action potential rhythm as the only parameter for the information flowing to and from each neuron. Such a strategy seems to be in contrast with novel experimental results [44, 48], since neurons are able to generate action potentials which are based on the input spike timings, with a precision up to 1 ms. The spike-timing synchrony is a natural effect that permits a neuron to be activated in correspondence with synchronous input spikes, while the neuronal activation of the post-synaptic neuron is negligible if pre-synaptic spikes arrives asynchronously to the target neuron. Axonal delays usually lie in the range 0.1 ms–44 ms, depending on the type and location of the neuron inside the network. Such a property becomes an important feature for the selection of the neural groups. The selection of neural groups is the result of the variation of synaptic connection according to the STDP rule. If a spike coming from an excitatory pre-synaptic neuron causes the firing of the post-synaptic neuron, the synaptic connection is reinforced since it gives the possibility of generating another spike in order to propagate the signal. Otherwise the synaptic connection is weakened. The values of the STDP parameters are chosen in order to permit a weakening that is greater than the reinforcement. Such a strategy permits the progressive removal of the unnecessary connections and the persistence of the connections between correlated neurons.

3.4.3. Architecture design. On the basis of the approach followed by Izhikevich [48], the CANN architecture design is inspired by the anatomical structure found in the mammalian cortex. In respect to the total number (N) of neurons, a percentage equal to 80% consists of excitatory neurons, while the remaining 20% are inhibitory neurons. A single CANN of 1000 artificial neurons consisting of 200 inhibitory neurons and 800 excitatory neurons was implemented. Cortical pyramidal neurons showing a regular spiking (RS) behavior were adopted for the excitatory subsection, corresponding to the following values for the Izhikevich neuron model: $a = 0.02, b = 0.2, c = -65, d = 8$ [43]. Inhibitory neurons have been simulated adopting the model of the cortical interneurons which exhibits a fast spiking (FS) property: $a = 0.1, b = 0.2, c = -65, d = 2$) [43]. Each neuron is connected to M different neurons in order to obtain a connection probability (M/N) equal to 0.1, but inhibitory neurons are connected only to excitatory neurons. Moreover, the synaptic weights of the connections arising from the inhibitory neurons remain unchanged during the learning process, while those regarding the connections from the excitatory neurons change according to the STDP rule. Axonal delays are fixed in the range between 1 ms and 20 ms. The time resolution has been set to 1 ms. The single rows of the input data set are dispatched to a subset of the excitatory neurons.

As the application starts, all the connections have the same synaptic weight. The network needs many seconds to get stabilized through depression and strengthening of the synaptic weights. During this first phase, the network shows the presence of a high amplitude rhythm, with a frequency in the range between 2 Hz and 4 Hz (delta waves). After a few hours of network activity, the spiking rhythm becomes uncorrelated and frequencies in the range between 30 Hz and 70 Hz appear (gamma waves). The occurrence of such rhythms is called pyramidal-interneuron network gamma (PING) and it seems to be related to the spikes of the pyramidal cells which excite the inhibitory interneurons. Such interaction allows a mutual inhibition which temporarily switches off the network activity. As the network becomes stable, the oscillation rhythm is assessed in the frequency range between 2 Hz and 7 Hz and the training phase is ended. We noticed the presence of a large number of neural groups, each of them able to perform a reproducible spike sequence with a precision of 1 ms. A labeling procedure allows one to associate a specific pattern to a neural group. Each stimulus that is used as an input pattern is able to select one group inside the network, showing that the network is able to perform a classification task.

4. Experimental results

4.1. Application to the e-nose

The e-nose was used to analyze the headspace of certified olive oil samples. A trained panel test assessed 60 olive oil samples from different regions (Tuscany, Apulia and Sicily) classified by an official panel test as extra virgin, virgin and defective. Classes were denoted as ExVg, Vg, Df, respectively. With the aim of replicating the experiment three times, 180 vials (volume 125 ml) were prepared by pouring 10 ml of each of the 60 olive oil samples in three vials, sealing and then waiting a few hours for equilibration. Three series of measurements were performed for each vial at the same environmental conditions, for a total of 540 experiments. The headspace of each vial was conveyed using a gas carrier (nitrogen) with a flow rate of 200 ml min^{-1} into the exposure chamber where the sensor array was lodged. The experimental protocol consisted

Table 1. Mean percentages of the confusion matrix.

	ExVg		Vg		Df	
	MLP	KSOM	MLP	KSOM	MLP	KSOM
ExVg	63.6	93.9	32.6	4.5	3.8	1.6
Vg	22.5	13.9	67.2	82.5	10.3	3.6
Df	2.2	0.0	21.0	3.2	76.8	96.8
	FKSOM	CANN	FKSOM	CANN	FKSOM	CANN
ExVg	95.0	97.8	3.8	2.2	1.2	0.0
Vg	12.7	1.6	83.8	96.1	3.5	2.3
Df	1.9	0.0	4.4	0.3	93.7	99.7

of 100 samplings of baseline acquisition, 400 samplings of exposure and 200 samplings of desorption. Sensor responses were sampled with a scan rate of 0.1 s.

The above-reported pattern recognition techniques and the proposed CANN were trained in order to classify the olive oil samples in terms of their quality. In order to check the generalization capability of the neural networks, a *k*-fold cross-validation was carried out. Cross-validation is one of several approaches for estimating the performance of a model on future as-yet-unseen data. In *k*-fold cross-validation, the original data set is partitioned into *k* subsets. For each cross-validation step, a single subset is retained as the test set, and the remaining $k-1$ subsets are used as a training set. The cross-validation process is then repeated *k* times, with each of the *k* subsets used exactly once as the test set. The *k* results from the folds then can be averaged (or otherwise combined) to produce a single estimation. In this work a 5-fold cross-validation was applied; each fold consisted of randomly selected samples, at least one for each category index was included in each fold.

A topological analysis of the KSOM and the FKSOM shows in each test the presence of minimally overlapping zones. In order to quantify results obtained in the cross-validation, a labeling process for the KSOM, the FKSOM and the CANN, and a test process for the MLP allowed samples to be classified as belonging to at least one of the three classes. Table 1 summarizes the mean percentages of the confusion matrix resulting from the cross-validation procedure.

As can be noticed, the MLP shows the worst performances, while the CANN is proved to exhibit the best performance. As expected [31], KSOM is able to classify ExVg, Vg and Df classes with accuracy rates respectively of 93.9%, 82.5% and 96.8%, while the FKSOM has 95.0%, 83.8% and 93.7%. The CANN performances are respectively 97.8%, 96.1% and 99.7%, showing a mean performance increase of 7.0% in comparison with the KSOM and of 7.7% in comparison with the FKSOM. But the best performances can be underlined in terms of misclassification, i.e. when a sample is classified as another one. In this case, the CANN performances get better up to 32%, in comparison with the MLP misclassification (ExVg misclassified as Vg), and up to 13% and 12%, in comparison respectively with the KSOM and FKSOM misclassification (Vg misclassified as ExVg).

Table 2. Mean recognition percentages for glucose (G), sodium dehydrocholate (SD), sodium chloride (SC), citric acid (CA) and glutamic acid (GA).

	MLP	KSOM	FKSOM	CANN
G	56.3	68.5	65.8	86.3
SD	65.0	75.2	70.1	91.9
SC	78.2	90.8	89.1	95.2
CA	75.4	92.2	93.0	99.5
GA	67.8	83.2	85.1	94.8

4.2. Application to the e-tongue

The e-tongue was used to analyze five compounds with different chemical characteristics (a carbohydrate, two salts, a weak organic acid and an amino acid) able to elicit different kinds of gustative perceptions (glucose at 0.1 M, sodium dehydrocholate at 0.01 M, sodium chloride at 0.1 M, citric acid at 0.5 M and glutamic acid at 0.06 M), representing the five classic tastes. Measurements were performed at concentration levels chosen so as to fit the human range of sensitivities. Over one hundred measurements were carried out over a four month period. As regards the KSOM and the FKSOM a topological analysis showed the presence of minimally overlapping zones for each test. In order to quantify results obtained in the cross-validation, a labeling process for the KSOM, the FKSOM and the CANN, and a test process for the MLP allowed samples to be classified as belonging to at least one of the five classes. Mean recognition percentages are summarized in table 2.

Also in the e-tongue, the MLP shows the worst performances, while the CANN is proved to exhibit the best performance. The CANN mean performances arise in comparison with the MLP, the KSOM and the FKSOM, respectively up to 25.0%, 11.6% and 12.9%.

5. Conclusions

Can mammalian cortex models enhance the recognition of patterns in artificial implementations of biological systems? Yes, they can. In this paper the pattern recognition module of an e-nose and e-tongue was implemented respectively by a cortical-based artificial neural network, a multilayer perceptron, a Kohonen self-organizing map and a fuzzy Kohonen self-organizing map. In particular, in the cortical-based artificial neural network, an artificial neuron model and a learning strategy with high computational efficiency and biological accuracy were adopted. The networks were singularly described and applied in the classification task of large datasets coming from a conducting poly(alkoxy-bithiophenes) sensor-based e-nose and a composite array-based e-tongue. The comparison of results showed that the cortical-based artificial neural network is able to enhance the recognition percentages of both the e-nose and the e-tongue in terms of classification and misclassification, successfully demonstrating the improvement of the performances.

References

[1] Osada Y and De Rossi D (ed) 2000 *Polymer Sensors and Actuators* (Berlin: Springer)

[2] Persaud K and Dodd G 1982 Analysis of discrimination mechanisms in the mammalian olfactory system using a model nose *Nature* **299** 352–5

[3] Pearce T C, Schiffman S S, Nagle H T and Gardner J W (ed) 2002 *Handbook of Machine Olfaction: Electronic Nose Technology* (Weinheim, Germany: Wiley-VCH)

[4] White J, Kauer J S, Dickinson T A and Walt D R 1996 Rapid analyte recognition in a device based on optical sensors and the olfactory system *Anal. Chem.* **68** 2191–202

[5] Ping W, Qingjun L, Wei Z, Hua C and Ying X 2007 The design of biomimetic artificial nose and artificial tongue *Sensors Mater.* **19** 309–23

[6] Persaud K C, Wareham P, Pisanelli A M and Scorsone E 2005 Electronic nose—new condition monitoring devices for environmental applications *Chem. Senses* **30** 252–3

[7] Ryan M A, Zhou H, Buehler M G, Manatt K S, Mowrey V S, Jackson S P, Kisor A K, Shevade A V and Homer M L 2004 Monitoring space shuttle air quality using the Jet Propulsion Laboratory electronic nose *IEEE Sensors J.* **4** 337–47

[8] Gardner J and Yinon J (eds) 2004 *Electronic Noses and Sensors for the Detection of Explosives (NATO Science Series II: Mathematics, Physics and Chemistry)* (Berlin: Springer)

[9] Rong L, Ping W and Wenlei H 2000 A novel method for wine analysis based on sensor fusion technology *Sensors Actuators* B **66** 246–50

[10] Ampuero S and Bosset J O 2003 The electronic nose applied to dairy products: a review *Sensors Actuators* B **94** 1–12

[11] Garcia-Gonzalez D L, Barie N, Rapp M and Aparicio R 2004 Analysis of virgin olive oil volatiles by a novel electronic nose based on a miniaturized SAW sensor array coupled with SPME enhanced headspace enrichment *J. Agric. Food Chem.* **52** 7475–9

[12] Logrieco A, Arrigan D W M, Brengel-Pesce K, Siciliano P and Tothill I 2005 DNA arrays, electronic noses and tongues, biosensors and receptors for rapid detection of toxigenic fungi and mycotoxins: a review *Food Additives Contam.* **22** 335–44

[13] Shykhon M E, Morgan D W, Dutta R, Hines E L and Gardner J W 2004 Clinical evaluation of the electronic nose in the diagnosis of ear, nose and throat infection: a preliminary study *J. Laryngol. Otol.* **118** 706–9

[14] Miekisch W, Schubert J K and Noeldge-Schomburg G F E 2004 Diagnostic potential of breath analysis: focus on volatile organic compounds *Clin. Chim. Acta* **347** 25–39

[15] Di Francesco F, Ceccarini A, Trivella M G and Fuoco R 2005 Breath analysis: trends in techniques and clinical applications *Microchem. J.* **79** 405–10

[16] Phillips M, Cataneo R N, Cheema T and Greenberg J 2004 Increased breath biomarkers of oxidative stress in diabetes mellitus *Clin. Chim. Acta* **344** 189–94

[17] Phillips M, Cataneo R N, Ditkoff B A, Fisher P, Greenberg J, Gunawardena R, Kwon C S, Rahbari-Oskoui F and Wong C 2003 Volatile markers of breast cancer in the breath *Breast J.* **9** 184–91

[18] Phillips M, Cataneo R N, Cummin A R C, Gagliardi A J, Gleeson K, Greenberg J, Maxfield R A and Rom W N 2003 Detection of lung cancer with volatile markers in the breath *Chest* **123** 2115–23

[19] Machado R F *et al* 2005 Detection of lung cancer by sensor array analyses of exhaled breath *Am. J. Respir. Crit. Care Med.* **171** 1286–91

[20] Phillips M *et al* 2004 Prediction of heart transplant rejection with a breath test for markers of oxidative stress *Am. J. Cardiol.* **94** 1593–4

[21] Di Natale C, Macagnano A, Davide F, D'Amico A, Legin A, Vlasov Y, Rudnitskaya A and Selezenev B 1997 Multicomponent analysis on polluted waters by means of an electronic tongue *Sensors Actuators* B **44** 423–8

[22] Toko K 1996 Taste sensors with global selectivity *Mater. Sci. Eng.* C **4** 69

[23] Vlasov Y, Legin A and Rudnitskaya A 1997 Cross-sensitivity evaluation of chemical sensors for electronic tongue: determination of heavy metal ions *Sensors Actuators* B **44** 532–7

[24] Vlasov Y, Legin A, Rudnitskaya A, D'Amico A and Di Natale C 2000 Electronic tongue—new analytical tool for liquid analysis on the basis of non-specific sensors and methods of pattern recognition *Sensors Actuators* B **65** 235–6

[25] Winquist F, Wide P and Lundström I 1997 An electronic tongue based on voltammetry *Anal. Chim. Acta* **357** 21–31

[26] Ping W and Jun X 1996 A Novel recognition method for electronic nose using artificial neural network and fuzzy recognition *Sensors Actuators* B **37** 169–74

[27] Gutierrez-Osuna R 2002 Pattern analysis for machine olfaction: a review *IEEE Sensors J.* **2** 189–202

[28] Panigrahi S, Balasubramanian S, Gu H, Logue C and Marchello M 2006 Neural-network-integrated electronic nose system for identification of spoiled beef *LWT—Food Sci. Technol.* **39** 135–45

[29] Yates J W T, Chappell M J, Gardner J W, Dow C S, Dowson C, Hamood A, Bolt F and Beeby L 2005 Data reduction in headspace analysis of blood and urine samples for robust bacterial identification *Comput. Methods Programs Biomed.* **79** 259–71

[30] Pavlou A K, Magan N, Meecham Jones J, Brown J, Klatser P and Turner A P F 2004 Detection of Mycobacterium tuberculosis (TB) in vitro and in situ using an electronic nose in combination with a neural network system *Biosens. Bioelectron.* **20** 538–44

[31] Pioggia G, Ferro M and Di Francesco F 2007 Towards a real-time transduction and classification of chemo-resistive sensor array signals *IEEE Sensors J.* **7** 237–44

[32] Pioggia G, Di Francesco F, Marchetti A, Ferro M and Ahluwalia A 2007 A composite sensor array impedentiometric electronic tongue: part I. Characterization *Biosens. Bioelectron.* **22** 2618–23

[33] Lonergan M C, Severin E J, Doleman B J, Beaber S A, Grubb R H and Lewis N S 1996 Array-based vapor sensing using chemically sensitive carbon black-polymer resistors *Chem. Mater.* **8** 2298–312

[34] Pioggia G, Tassoni L, Mazzoldi A, Bertarelli C, Di Francesco F and De Rossi D 2006 Preparation and characterization of conducting chemo-sensitive layers based on polythiophenes *Meas. Sci. Technol.* **17** 3265–71

[35] Brereton R 2003 *Chemometrics. Data Analysis for the Laboratory and Chemical Plant* (Chichester: Wiley)

[36] Goodner K, Dreher G and Rouseff R 2001 The dangers of creating false classifications due to noise in electronic nose and similar multivariate analyses *Sensors Actuators* B **80** 261–6

[37] KinneBrock W 1992 *Neural Networks* (Munchen: Oldenburg Verlag)

[38] Kohavi R and Provost F 1998 Glossary of terms *Mach. Learn.* **30** 271–4

[39] Kohonen T 1997 *Self-Organising Maps* 2nd edn (*Springer Series in Information Sciences* vol 30) (New York: Springer)

[40] Chen-Kuo Tsao E, Bezdek J C and Pal N R 1994 Fuzzy Kohonen clustering networks *Pattern Recognit.* **27** 757–64

[41] Marcelloni F 2003 Feature selection based on a modified fuzzy C-means algorithm with supervision *Inf. Sci.* **151** 201–26

[42] Izhikevich E M 2004 Which model to use for cortical spiking neurons? *IEEE Trans. Neural Netw.* **15** 1063–70

[43] Izhikevich E M 2003 Simple model of spiking neurons *IEEE Trans. Neural Netw.* **15** 1569–72
[44] Edelman G M 1987 *Neural Darwinism: The Theory of Neuronal Group Selection* (New York: Basic Books)
[45] Hodgkin A L and Huxley A F 1952 A quantitative description of membrane current and its application to conduction and exitation in nerve *J. Physiol.* **117** 500–44
[46] Morris C and Lecar H 1981 Voltage oscillations in the barnacle giant muscle fiber *Biophys. J.* **35** 193–213
[47] FitzHugh R 1961 Impulse and physiological states in models of nerve membrane *Biophys. J.* **1** 445–66
[48] Izhikevich E M, Gally J A and Edelman G M 2004 Spike-timing dynamics of neural groups *Cerebral Cortex* **14** 933–44